



Protonation and methylation of thiophenol, thioanisole and their halogenated derivatives: mass spectrometric and computational study

Pham-Cam Nam^{a,c}, Robert Flammang^{b,*}, Hung Thanh Le^{a,d},
Pascal Gerbaux^{b,1}, Minh Tho Nguyen^{a,2}

^a Department of Chemistry, University of Leuven, Celestijnenlaan 200F, B-3001 Leuven, Belgium

^b Laboratoire de Chimie Organique, Université de Mons-Hainaut, Avenue Maistriau 19, B-7000 Mons, Belgium

^c Faculty of Chemical Engineering, University of Danang, Danang, Viet Nam

^d Group of Computational Chemistry, Faculty of Chemical Engineering,
HoChiMinh City University of Technology, Ho Chi Minh City, Viet Nam

Received 17 October 2002; accepted 14 March 2003

Dedicated to Professor Helmut Schwarz, on the occasion of his 60th birthday, for his outstanding contributions to mass spectrometry.

Abstract

The protonation and methylation of thiophenol (C_6H_5SH), thioanisole ($C_6H_5SCH_3$) and 4-bromo derivatives have been studied using both tandem mass spectrometric techniques and ab initio quantum chemical calculations. Protonated 4-bromo thio-compounds produced by chemical ionization (CI) are found to be collisionally dehalogenated in an rf-only quadrupole collision cell in the low (20–30 eV) kinetic energy regime giving essentially thiophenol or thioanisole radical cations. This is indicated by MS/MS/MS experiments performed in an hybrid sector-quadrupole-sector mass spectrometer. B3LYP and CCSD(T) calculations using the 6-311++G(d,p) basis set consistently confirm that protonation of either (bromo)thiophenol or thioanisole takes place on the ring; the C_4 -protonated thiophenol lies about 13 kJ mol^{-1} below the S-protonated isomer. However, under similar conditions, protonated thioanisole is also readily demethylated generating thiophenol radical cation, but no isomer has been detected. On the other hand, experimental and theoretical results reveal a regiospecific cationization (methylation) at the sulfur atom of the title compounds. The proton and methyl cation affinities are estimated as follows: PA (thiophenol) = $812 \pm 10 \text{ kJ mol}^{-1}$, MCA (thiophenol) = $397 \pm 10 \text{ kJ mol}^{-1}$, PA (thioanisole) = $839 \pm 10 \text{ kJ mol}^{-1}$, and MCA (thioanisole) = $454 \pm 10 \text{ kJ mol}^{-1}$. The available experimental value of 873 kJ mol^{-1} for PA (thioanisole) appears to be overestimated. Calculated PAs at various sites of halogeno (F, Cl and Br) thiophenols (*o*, *m*, *p*) are also reported.

© 2003 Elsevier Science B.V. All rights reserved.

Keywords: Thiophenols; Chemical ionization; Collisional activation; Molecular orbital calculations; Proton and methyl cation affinities

* Corresponding author. Tel.: +32-65-373342;

fax: +32-65-373515.

E-mail addresses: robert.flammang@umh.ac.be (R. Flammang),
minh.nguyen@chem.kuleuven.ac.be (M.T. Nguyen).

¹ Postdoctoral researcher of the Fonds national de la recherche scientifique.

² Co-corresponding author.

1. Introduction

The importance of sulfur-containing compounds in biological systems as well as in atmospheric and environmental chemistry is now well established [1,2]. Since the thiol group (R-SH) could easily be oxidized,

especially in the presence of light, they have been used as efficient antioxidants of organic matter ranging from polymers to living cell systems [1,2]. In this regard, aromatic thiols (Ar-SH) that have the pK_a values ranging from 4 to 7 have been shown to be effectively more reactive than aliphatic thiols (R-SH) of similar pK_a s [3]. In view of such interesting properties, the elementary reactions of the antioxidant actions of aryl thiols and the characterization of the resulting intermediates including the thiophenol radical cations ($RSH^{\bullet+}$) and thiyl radicals (RS^{\bullet}), have been the subject of numerous experimental and theoretical studies [3–12]. In some cases, a simultaneous occurrence of homolysis and single electron transfer in the processes has been observed [12]. The oxidation of thioanisole (Ph-S-Me) has also been found to be of potential use in the decontamination of toxic chemicals [13,14]. On the other hand, the addition of a thiophenol to an electron-deficient and prochiral alkene, forming an adduct having a new C–S chemical bond with a high level of diastereoselectivity, constitutes a key reaction in biosynthesis and chemical synthesis of biologically potent compounds [15].

In contrast, relatively little is known about the reactivity of thiophenols with respect to electrophilic agents. In a 1983 mass spectrometric study, Woods et al. [16] determined the site of gas phase attachment of the methyl cation to thiophenol on the basis of the characteristic fragmentations of the mass-selected adduct ions and the relevant MS/MS spectra of the ion–molecule reactions. It appeared that thiophenol is methylated, almost exclusively (>90%), at the sulfur atom, in clear-cut difference with phenol (Ph-OH), where a competitive ring and oxygen protonation or alkylation were observed [16,17]. Recently, experimental [18] and theoretical [19] studies further demonstrated that protonation of phenol actually takes place both at the benzene ring carbon and oxygen atoms. Even though proton attachment to the C_4 -carbon turns out to be the more dominant process, the oxygen-protonated species has been detected [18] thanks to the large energy barriers connecting different protonated forms [19].

In this paper, we set out to determine the proton and methyl cation affinities and the reactive sites of thiophenol, thioanisole and their mono-bromo derivatives using both experimental tandem mass spectrometric techniques and quantum chemical computations. For the sake of comparison, some calculations on various fluorinated and chlorinated thiophenols ($X-C_6H_4SH$ with $X = F, Cl$) have also been performed. Recently, we used the same combined experimental and theoretical approach to investigate the protonation and subsequent processes of various aromatic compounds, including phenols and anisoles [19,20], benzonitrile [21], aniline [22], benzaldehyde [23], and pyridines [24].

2. Experimental and theoretical methods

The mass spectrometric experiments were performed on a large scale (Micromass AutoSpec 6F, Manchester) tandem mass spectrometer having a $E_1B_1E_2qcE_3B_2cE_4$ geometry, where E stands for electric sector, B for magnetic sector, q for an rf-only quadrupole collision cell and c for the collision cells used in the present work [25,26]. Typical conditions were 8 kV accelerating voltage, 1 mA emission current (in the chemical ionization (CI) mode), 200 μ A trap current (in the electron ionization mode) and 70 eV ionizing electron energy.

The installation of an rf-only quadrupole collision cell (Qcell) inside the instrument between E_2 and E_3 has also been reported elsewhere [26]. This modification allows the study of associative ion–molecule reactions and the study of collisional activation of decelerated ions. The experiments utilizing the Qcell consist of the selection of a beam of fast ions (8 keV) with $E_1B_1E_2$ and the deceleration of these ions to approximately 20–30 eV. The interaction between the ions and argon collision gas (the pressure of the gas is estimated to be about 10^{-3} Torr) is thereafter realized in the Qcell and, after re-acceleration at 8 keV, all the ions generated in the quadrupole are separated and mass measured by scanning the field of the second magnet.

The *high energy* CA spectra of mass-selected ions generated in the Qcell have been recorded by scanning the field of E_4 after collisional activation (nitrogen) in the last collision cell.

All the compounds considered in this work were commercially available (Aldrich) and were used without any further purification.

In order to quantitatively evaluate the differences, on one hand between protonation and methylation and on the other hand between thiophenols and thioanisoles, we have carried out *ab initio* calculations on the parent and simple halogeno-substituted systems. All calculations were performed with the Gaussian 98 set of programs [27]. Geometrical parameters of the structures considered were initially optimized and subsequently characterized by harmonic vibrational analyses using the density functional theory (DFT) with the popular hybrid B3LYP functionals [28] in conjunction with the dp-polarized 6-31G(d,p) basis set. The zero-point energy corrections (ZPE) to relative energies were also obtained at this level. Geometries of the relevant stationary points were then reoptimized making use of the same method but with the larger 6-311++G(d,p) basis set including diffuse functions. In order to further verify the validity of the B3LYP relative energies, electronic energies were calculated for the protonated thiophenol forms at the coupled-cluster CCSD(T) level of molecular orbital theory using the 6-311++G(d,p) basis set and B3LYP/6-311++G(d,p) geometries. Throughout this section, bond distances are given in angstroms, bond angles in degrees and relative energies in kJ mol^{-1} . Unless otherwise noted, the latter values are derived from B3LYP/6-311++G(d,p) + ZPE calculations.

3. Results and discussion

3.1. Protonation of thiophenol

The collisional activation (CA) mass spectrum of the molecular ions of thiophenol (m/z 110) produced by electron ionization (EI) of neutral thiophenol is

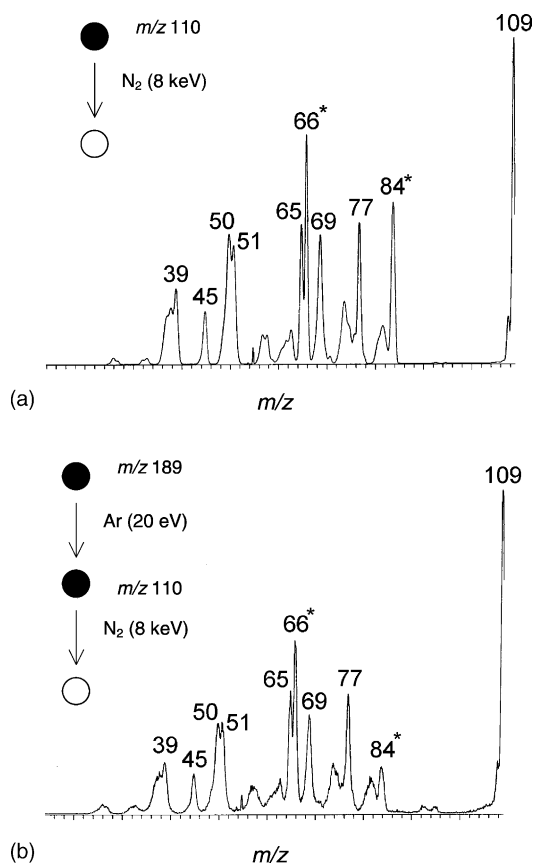
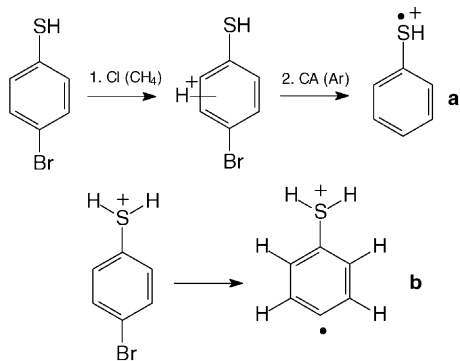


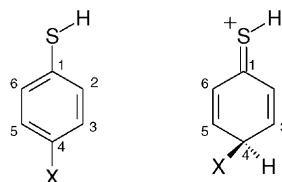
Fig. 1. CA ($\text{N}_2/8\text{ keV}$) spectra of (a) the molecular ions of thiophenol (m/z 110) and (b) the $[\text{M} + \text{H} - \text{Br}]^{+\bullet}$ ions of protonated 4-bromothiophenol; asterisk indicates the peaks observed without the presence of the collision gas. The terminology used to schematize the ion–molecule interactions is that introduced by Schwartz et al. [35]: a filled circle represents a fixed (or selected) mass; an open circle, a variable (or scanned) mass, whereas the neutral reagent that causes the mass transition is shown between the circles.

shown in Fig. 1a. This spectrum will be used as a reference spectrum all along this work. The most intense peaks observed at m/z 84 and 66 (corresponding to the losses of ethyne and carbon monosulfide, respectively) are the reactions already observed without the presence of a collision gas and then result from unimolecular rearrangements of the metastable molecular ions. Thiophene and cyclopentadiene ions (m/z 84: m/z 66 = 0.83) are likely to be generated in these “slow” reactions.



Scheme 1.

The second spectrum displayed in Fig. 1b has been recorded after protonation of 4-bromothiophenol under methane CI and collision-induced debromination of the so-produced ions with argon in the quadrupole collision cell. Such a protonation–dehalogenation sequence was expected to produce the “conventional” thiophenol ions **a** in the case of ring carbon protonation (steps 1 and 2 in Scheme 1) or the distonic ions **b** in the case of sulfur protonation. Actually, the so-produced m/z 110 ions exhibit the thiophenol structure as evidenced by the identical collision-induced dissociations displayed in the MS/MS/MS spectrum (Fig. 1b) and in the reference CA spectrum (Fig. 1a). Some significant differences are only detected for the reduced abundance of the unimolecular reactions (mainly for the m/z 84 ions) suggesting a broader distribution of internal energies in the direct EI process as compared with the CI ionization. Because unimolecular processes are too sensitive to the energy content of the ions prior to the collision, it is of usual practice to “forget” these reactions when comparing CA spectra [29]. These experimental observations indicate that the preferential site of protonation of 4-bromothiophenol is probably a ring carbon atom rather than the sulfur atom since the consecutive debromination step regenerates almost exclusively the “conventional” thiophenol ion **a**. Structural significant peaks are indeed observed at m/z 77/51 for phenyl cations. Intense peaks at m/z 76/50 (benzyne ions) are expected for the isomeric distonic radical cations **b**. Such benzyne ions



Scheme 2.

have been previously detected for distonic isomers of aniline, benzonitrile... [20–23]. It is expected that the site of protonation of thiophenol is also a ring carbon atom as for the 4-bromothiophenol molecule (cf. Scheme 2); this will be proved by theoretical ab initio calculations (vide infra). At this point of the discussion, it is worth noting that the distonic form **b** seen in Scheme 1, is calculated to be 219 kJ mol^{-1} higher in energy than the ionized thiophenol **a**. In the neutral state, the energy gap between both forms amounts to 487 kJ mol^{-1} . The ionized thio forms having a C=S bond are found to be more stable than **b**, being about $70\text{--}100 \text{ kJ mol}^{-1}$ less stable than **a**.

Table 1 lists the calculated proton affinities (PAs) of thiophenol using two distinct quantum chemical methods, namely the density functional theory with the popular hybrid B3LYP functional and the molecular orbital coupled-cluster CCSD(T) method, in conjunction with the 6-311++G(d,p) atomic basis. Recent theoretical studies [30–32] on similar systems demonstrated that the B3LYP method provides relative energies comparable to those derived from the molecular orbital coupled-cluster theory and that the resulting absolute deviations between B3LYP and CCSD(T) values, when using the same basis set, amount to an average of about 10 kJ mol^{-1} .

The PAs of thiophenol at four different positions are shown in Table 1. The values, obtained by both theoretical methods, are comparable to each other with the largest deviation of 14 kJ mol^{-1} for the sulfur atom PAs. More important perhaps is the fact that the ring-protonation at the C₄ position is clearly favored over the S-protonation by up to 13 or 28 kJ mol^{-1} [CCSD(T) and B3LYP values, cf. Scheme 2 for definition]. The PAs of *ortho*-carbons (C₂ and C₆) are

Table 1
Calculated proton affinities (kJ mol^{-1}) of thiophenol and calculated methyl cation affinities at different sites

Site ^a	Proton affinity ^b		Methyl affinity ^b
	B3LYP/6-311++G(d,p)	CCSD(T)/6-311++G(d,p)	B3LYP/6-311++G(d,p)
S	785	799	397
C ₂	799	797	374
C ₃	755	749	330
C ₄	813	812	388
C ₅	755	–	–
C ₆	799	–	–
C ₁ <i>ipso</i>	739	–	–

^a See Scheme 2 for definition of atom numbering.

^b Using B3LYP/6-311++G(d,p)-optimized geometries and ZPEs (scaled down by a uniform factor of 0.98).

similar to the PA(S) followed by those of *meta*-carbons (C₃ and C₅), whereas the *ipso*-carbon (C₁) is associated with the smallest value. Such an ordering of PAs is similar to that already calculated for phenol [19].

The B3LYP-optimized geometries of neutral thiophenol and both C₄- and S-protonated forms are shown in Fig. 2. The geometry of the neutral form is quite close to that of phenol [20]. The S-protonation

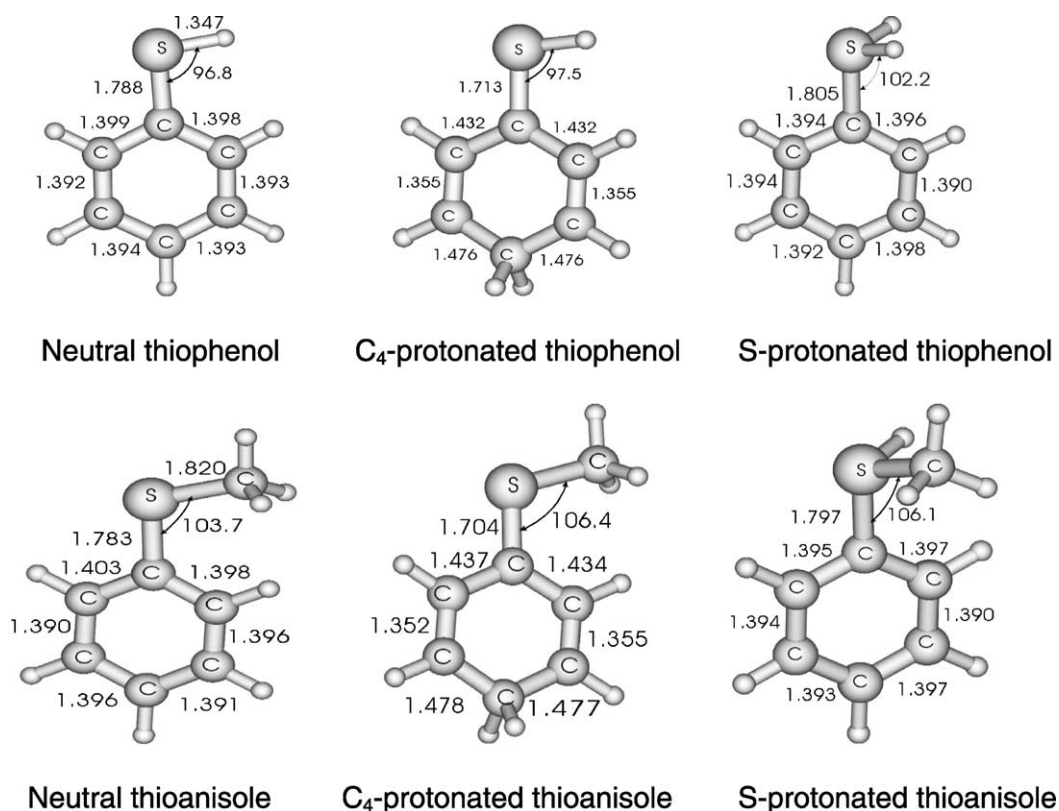


Fig. 2. Selected B3LYP/6-311++G(d,p)-optimized geometries of the neutral, C₄-protonated and S-protonated thiophenol (upper values) and thioanisole (lower values). Bond lengths are given in angstroms and bond angles in degrees.

slightly stretches the C–S distance (by 0.015 Å) and keeps the phenyl ring almost intact, whereas the C₄-protonation profoundly modifies the electronic structure of the ring. Indeed, the C₄-protonated form exhibits a quinoidic structure having one formal C=S and two C=C double bonds (C₂C₃ and C₅C₆ bonds), the positive charge residing on the sulfur atom.

To the best of our knowledge, there is no available experimental determination of the proton affinity of thiophenol. As seen in Table 1, both B3LYP and CCSD(T) methods provide two consistent values of 812 and 813 kJ mol⁻¹ for the PA(C₄) of thiophenol. In the case of the PA of phenol [19], both methods also yielded two almost identical values of 820 and 819 kJ mol⁻¹, respectively. These values compare quite well with the experimental estimates of 816–818 kJ mol⁻¹ [33]. In view of the similarity of the behavior of the methods employed as well as the molecular systems considered, it seems reasonable to suggest that the computed results are quite close to the true PA of thiophenol. In other words, the following value could be proposed: PA (thiophenol) = 812 ± 10 kJ mol⁻¹.

Compared with the values previously determined for phenol using the same methods [19], it appears that replacement of the –OH by the –SH group tends to significantly reduce the energy gap between both ring and hetero-atom protonation processes which goes from 77 kJ mol⁻¹ in phenol to 28 kJ mol⁻¹ in thiophenol. This is probably due to the higher ability of the sulfur atom to stabilize the formal positive charge.

In this first part, we assume, as far as the experimental observations are concerned, that the protonation site in thiophenol is the same as in 4-bromothiophenol. Actually, this latter molecule was needed in the protonation–debromination sequence of reactions. In the following part of this work, it will be confirmed, by theoretically studying the protonation of several halothiophenols, that this assumption was quite reasonable.

3.2. Proton affinities of halogenothiophenols

Table 2 records the PAs of a series of monohalogenated thiophenols determined using the same level of theory. The halogens including fluorine, chlorine and bromine (X = F, Cl, Br), are systematically introduced in the *ortho*, *meta* and *para* positions of the phenyl ring with respect to the SH group. No experimental PAs of these molecules were found in the literature.

For each substituted thiophenol, seven protonated forms have been considered. A number of interesting features emerge from results of Table 2:

- (i) For the *o*-X and *m*-X derivatives, the C₄ position is consistently the most attractive protonation site. The corresponding PAs are reduced relative to the parent unsubstituted thiophenol, ranging from 790 to 796 kJ mol⁻¹ for *o*-X to 804–808 kJ mol⁻¹ for *m*-X-thiophenols. The reductions and fluctuations of the sulfur atom PAs are smaller as they range from 761 to 769 kJ mol⁻¹. Within the ring, the C₆-protonation is however

Table 2
Calculated proton affinities of some halothiophenols (kJ mol⁻¹)^a

Protonation site ^b	X = F			X = Cl			X = Br		
	<i>o</i>	<i>m</i>	<i>p</i>	<i>o</i>	<i>m</i>	<i>p</i>	<i>o</i>	<i>m</i>	<i>p</i>
S	761	764	766	766	766	771	769	768	772
C ₂	730	788	772	752	793	775	766	795	778
C ₃	750	679	748	754	696	752	756	714	754
C ₄	790	804	747	793	807	764	796	808	781
C ₅	758	725	747	758	729	751	759	732	753
C ₆	776	798	772	781	799	776	784	801	778
C ₁ <i>ipso</i>	730	707	744	738	713	745	741	740	747

^a Using B3LYP/6-311++G(d,p)-optimized geometries and ZPEs (scaled down by a uniform factor of 0.98).

^b See Scheme 2 for definition of atom numbering.

calculated to be still favored over the S-protonation. In the *m*-X series, the maximum difference between C₄ and C₆ PAs amounts to 8 kJ mol⁻¹. It can thus be expected that additional substituents could easily tip the balance into a C₆-protonation, then becoming the most favored one. Both the C₃ and C₁ sites are much less accessible for electrophile attachment. The main effect caused when attaching a halogen atom in the *ortho* and *meta* positions is thus a small and uniform reduction of the PAs, the effect being more accentuated in *o*-X derivatives.

- (ii) Protonation at the site bearing the substituent is strongly disfavored. Indeed, when the X-atom resides on an *o*-position, the latter becomes less open for a proton attack as compared not only with the C₆ site, but also with both C₃ and C₅ sites. This holds true for a *m*-substitution and in particular for the *p*-substitution. In *p*-F- and *p*-Cl-thiophenols, the C₄-protonation is no longer the most preferred process. In this case, the C₂-protonation becomes the global protonation site, even though the S-protonation should also be accessible with a difference of only 4–6 kJ mol⁻¹. In the case of 4-bromothiophenol, the C₄ site remains the most basic one, but with quite small gaps relative to the C₂ (3 kJ mol⁻¹) and S (9 kJ mol⁻¹) sites.
- (iii) When the X-atom is attached in a *m*-position, an *o*-protonation occurs preferentially on the farther C₆ site rather than on the closer C₂ site. This results in a detectable effect, quantified from 6 to 10 kJ mol⁻¹, of the halogen on the adjacent centers.
- (iv) The C₄ protonation appears to be an intrinsic property of thiophenols. This is reinforced when the halogen is attached in a *meta* position, in such a way that both protonation and substitution sites are situated close each to other. In such a relative *ortho* disposition, the halogen atom could induce a stabilization of the excess positive charge on the adjacent center by allowing a better delocalisation of the sulfur lone pair into the ring. It can in fact be verified that, in

each series of X, the highest PA corresponds to the C₄-protonation of the 3-X-derivative: 804 kJ mol⁻¹ for *m*-fluorothiophenol, 807 kJ mol⁻¹ for *m*-chlorothiophenol and 808 kJ mol⁻¹ for *m*-bromothiophenol (cf. Table 2).

For the sake of comparison, we note that the protonation behavior of halothiophenols is essentially similar to that of the halophenol analogues [19]. In replacing oxygen in phenols by sulfur to form thiophenols, we uniformly reduce the PA(C₄)s by at most 10 kJ mol⁻¹, which is in the same order of magnitude as in the parent pair. The PA(S)s remain however about 30–40 kJ mol⁻¹ larger than for their oxygen counterparts.

3.3. Protonation of thioanisole

Thioanisole is readily protonated in the CI source using methane as the reagent gas. The protonation site of thioanisole could perhaps be identified by performing a subsequent collision-induced demethylation of the protonated molecule and identifying the so-produced radical cations. This sequence of reaction is, at least in principle, quite similar to the protonation–debromination experiment realized starting with 4-bromothiophenol.

The demethylation of protonated thioanisole is indeed found to be an efficient dissociation occurring in the quadrupole collision cell pressurized with argon. The recorded resulting spectrum is presented in Fig. 3a. The CA spectrum of the so-produced *m/z* 110 ions (cf. Fig. 3b and Fig. 1) indicates again the formation of thiophenol molecular ions **a** (Scheme 3).

At this point of the work, the crucial question is to know whether the protonation of thioanisole exclusively takes place at the sulfur atom as apparently suggested by the MS/MS/MS data. Theoretical results summarized in Table 3 point out that thioanisole protonation is parallel to that of thiophenol. Thanks to the methyl electron donation, the PA(S) is markedly increased by 50 kJ mol⁻¹ in going from thiophenol to thioanisole. However, even if the C₄-protonation seems to remain the most energetically favored attack, the 4 kJ mol⁻¹ difference between both PAs

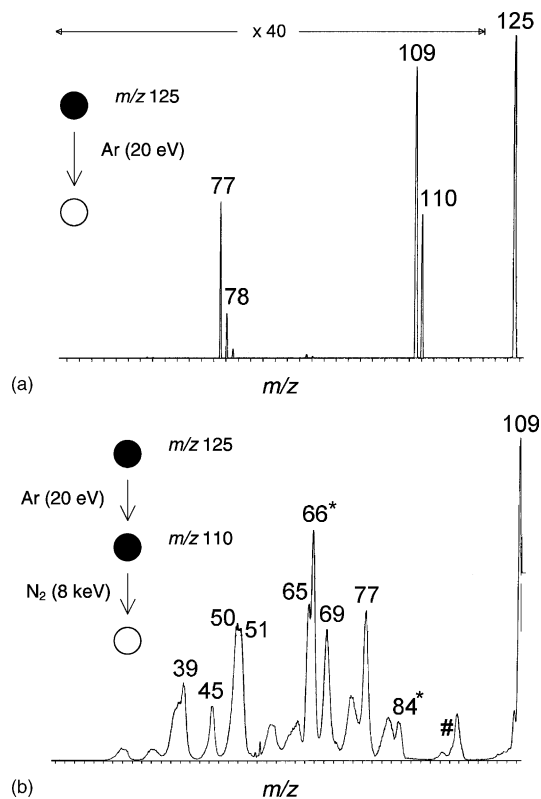
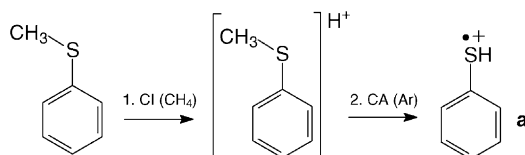


Fig. 3. (a) Low energy CA spectrum (Ar, 20 eV) of protonated thioanisole (m/z 125) and (b) CA spectrum ($N_2/8$ keV) of the $[M + H-CH_3]^+$ ions generated by collision-induced methyl loss from protonated thioanisole. (#) Artefact peaks; (*) peaks already observed without the presence of the collision gas.

calculated values (S- and C₄-protonations) is too small to derive unambiguous conclusions, especially because the protonation is realized in the CI source using the strong acidic methanonium ions. On the



Scheme 3.

other hand, the C₂ and C₃ sites are equally benefited from methyl donation, the corresponding PA values being increased by 27 and 18 kJ mol⁻¹, respectively (cf. Tables 1 and 3). The proton affinity at the C₄ carbon of thioanisole amounts to 839 kJ mol⁻¹ using B3LYP/6-311++G(d,p) calculations. The only available experimental estimate for this quantity is 873 kJ mol⁻¹ [33,34]. There is thus a markedly large discrepancy of 34 kJ mol⁻¹. In the cases of phenol and anisole, the calculated proton affinities computed at the same level of theory amount to 820 (experimental: 816–818 kJ mol⁻¹) and 841 kJ mol⁻¹, respectively. The PA enjoys thus an increase of 21 kJ mol⁻¹ following methylation at oxygen, a value comparable to that of 26 kJ mol⁻¹ in the case of methylation at sulfur. In other words, this value seems to represent a reasonable variation. We therefore believe that the available experimental value [33,34] of 873 kJ mol⁻¹ for the PA of thioanisole is significantly overestimated.

To obtain additional information on the relative stabilities of isomeric protonated thioanisole and the proton mobility within the cation, a portion of the (C₇H₉S)⁺ potential energy surface (PES) has been constructed at the B3LYP/6-311++G(d,p)+ZPE level and schematically displayed in Fig. 4. The energy

Table 3

Proton and methyl cation affinities (kJ mol⁻¹) of thioanisole and 4-bromothioanisole at different sites

Site ^a	Proton affinity ^b		Methyl affinity ^b
	Thioanisole	4-Bromothioanisole	Thioanisole
S	835	821	454
C ₄ <i>para</i>	839	813	423
C ₃ <i>meta</i>	773	771	356
C ₂ <i>ortho</i>	826	806	409
C ₁ <i>ipso</i>	–	758	–

^a See Scheme 2 for definition of atom numbering.

^b Using B3LYP/6-311++G(d,p)-optimized geometries and ZPEs (scaled down by a uniform factor of 0.98).

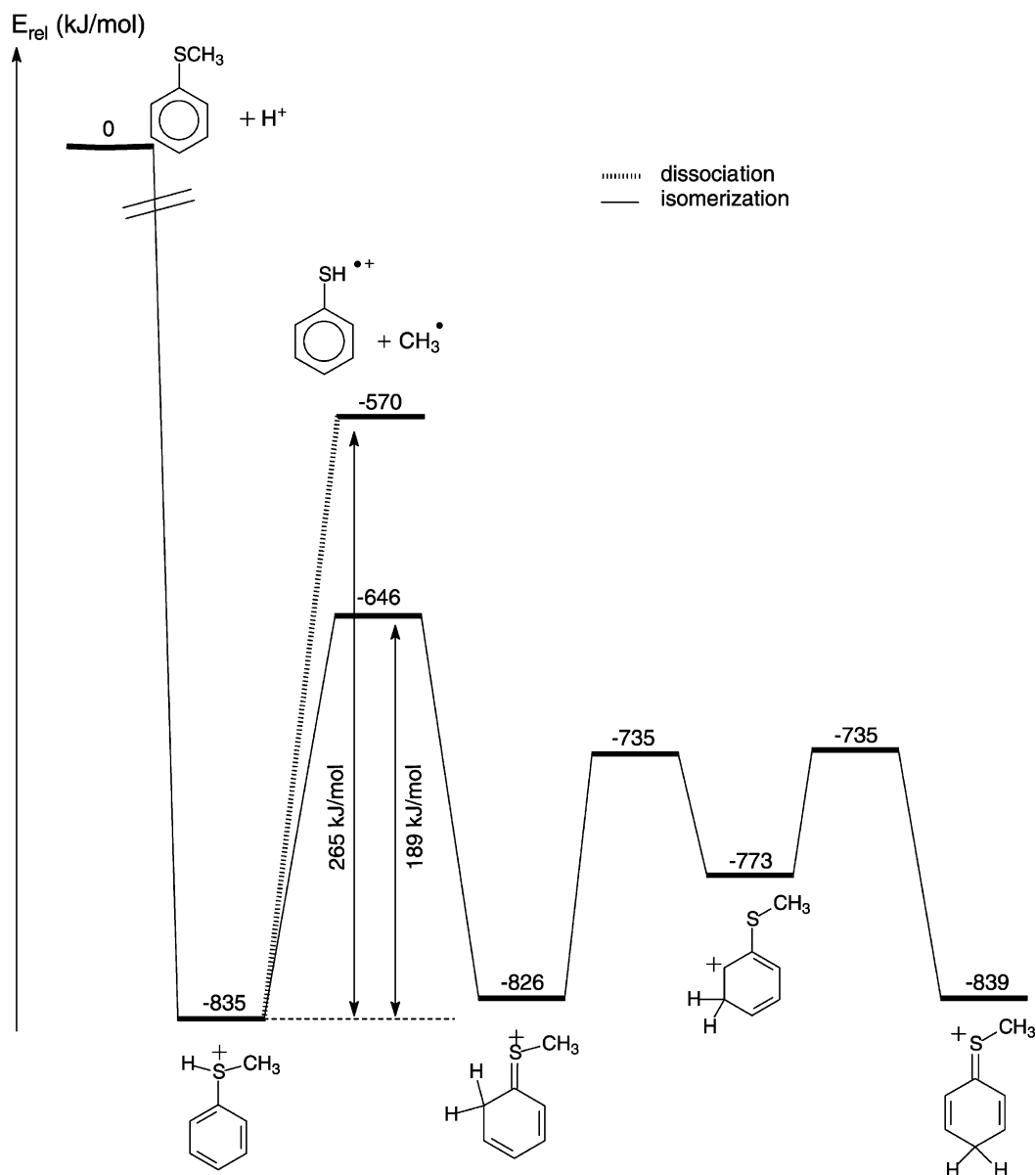


Fig. 4. Potential energy surface, obtained at the B3LYP/6-311++G(d,p)+ZPE level of theory, of the $C_7H_9S^+$ isomers of protonated thioanisole. The transition states corresponding to proton migrations are shown.

profile vividly illustrates that the migration of the excess proton between the various heavy atoms via three transition structures (TS) for 1,2- and 1,3-H shifts is a quite easy process. Starting from the C_3 -protonated form, the excess proton can migrate to give either the C_2 - or the C_4 -isomers by 1,2-H shifts overcoming

comparable energy barriers. From the C_2 -form, the TS for 1,2-H shift connecting the *ipso* C_1 -form could not be located. All attempts searching for a TS connecting C_1 - and C_2 -forms invariably led to a TS for 1,3-H shift linking the C_2 to the S-protonated form. The significant separation of the ring-protonated thioanisoles

from their S-protonated isomer could allow them to be separately detected, for example in low temperature matrix conditions, provided their individual productions can be achieved. Nevertheless, their inter-conversion appears realizable under the high energy conditions of our CA experiments. Indeed, thiophenol molecular ions are identified in the present experiment after collision-induced demethylation of the protonated species. This peculiar process requires about 265 kJ mol^{-1} starting from S-protonated thioanisole, see Fig. 4. This is significantly above the highest transition barrier for proton migration (189 kJ mol^{-1}), see Fig. 4. Such collision-induced rearrangement is probably responsible for the apparently exclusive demethylation of S-protonated form observed in the CA experiment. It is also important to emphasize that, under the protonation conditions used in this experiment, it is quite reasonable to expect a mixture of initially generated S- and C₄-protonated species.

3.4. Protonation of 4-bromothioanisole

To further probe the protonation site of thioanisole, we have carried out another series of experiments in which 4-bromothioanisole was first protonated under CI conditions and the resulting protonated species was subsequently subjected to a CA with argon. It turns out that the excited cations only undergo the loss of bromine. The CA spectrum of the so-produced ions, shown in Fig. 5b, is found very similar to the CA spectrum of ionized thioanisole (Fig. 5a) and again this points out the formation of the conventional radical cations **c** rather than the distonic ions **d** (Scheme 4). Again, in this system, the distonic radical cation **d** (Scheme 4) is calculated to be 205 kJ mol^{-1} higher in energy than the classical thioanisole ion **c**. Apparently, the observation of ionized thioanisole after the protonation–debromination sequence of reactions again suggests a predominant ring protonation.

To verify this finding, we have computed the PAs at various positions of 4-bromothioanisole and these theoretical results are summarized in Table 3. As in the case of thiophenols (vide supra), a significant reduction of the PAs upon bromination could

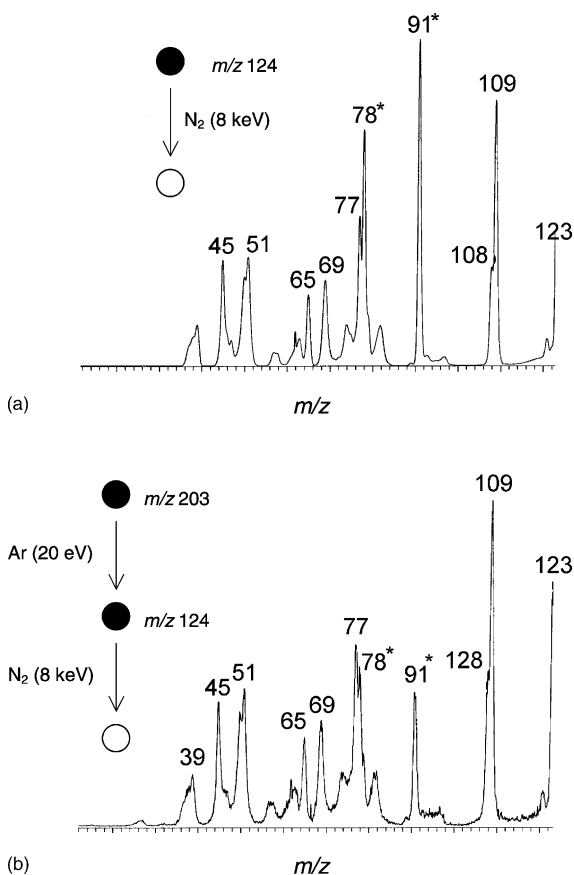
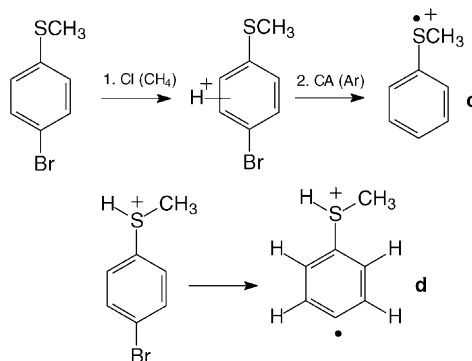


Fig. 5. CA ($\text{N}_2/8 \text{ keV}$) spectra of the molecular ions of thioanisole (m/z 124) (a) and of the $[\text{M}+\text{H}-\text{Br}]^{\bullet+}$ ions generated by collision-induced bromine loss from protonated 4-bromothioanisole (b). Asterisk indicates the peaks observed without the presence of the collision gas.



Scheme 4.

be noticed: 20 kJ mol^{-1} for C_2 , 14 kJ mol^{-1} for S and 26 kJ mol^{-1} for C_4 -PAs. These reductions are in the same order of magnitude to those obtained for the thiophenol–4-bromothiophenol pair (cf. Tables 1 and 2). Nevertheless, it turns out that, in this case, the S-protonation becomes slightly more favored than the C_4 -protonation (by 8 kJ mol^{-1}) followed by the

C_2 -protonation (15 kJ mol^{-1}). Within the expected accuracy of the level of theory employed, these structures could be regarded as having a comparable energy content.

More interesting perhaps is the ease with which the five protonated forms of 4-bromothioanisole may interconvert. Fig. 6 displays the potential energy profile

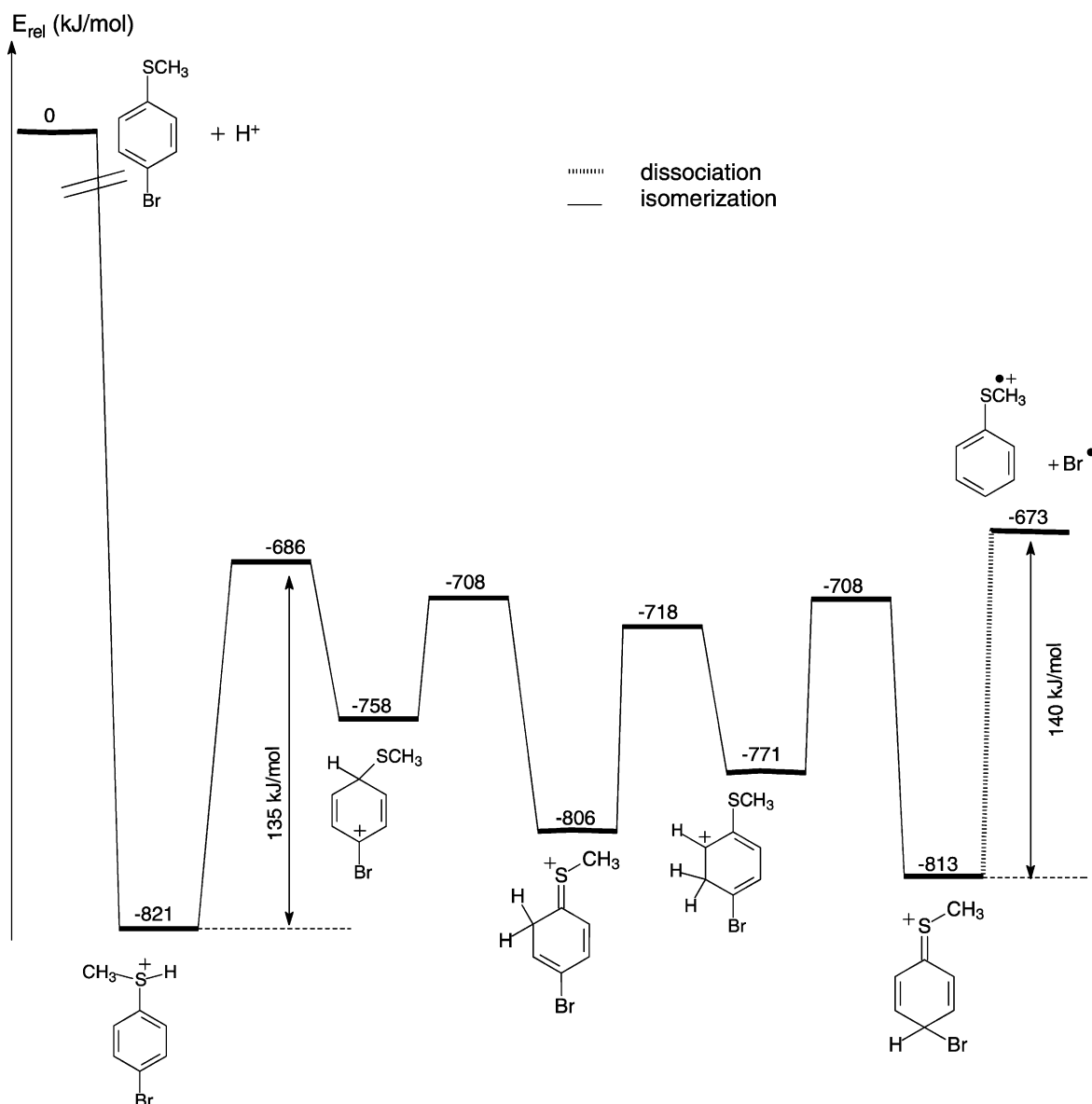


Fig. 6. Potential energy surface, obtained at the B3LYP/6-311++G(d,p) + ZPE level of theory, of the $\text{C}_7\text{H}_8\text{BrS}^+$ isomers of protonated 4-bromothioanisole. The transition states corresponding to proton migrations are shown.

schematically illustrating their connections through successive 1,2-proton migration. In this case, the *ipso* isomer can well be identified. Starting from the S-protonated form, an energy barrier of 135 kJ mol^{-1} is associated with the sulfur/ring carbon atom inter-conversion. That actually corresponds to a reduction of 54 kJ mol^{-1} from the parent thioanisole (cf. Fig. 4). These calculated results therefore point out that the formation of the radical cation **c** (148 kJ mol^{-1} relative to S-protonated thioanisole), see Scheme 4 and Fig. 6, can be due to a relatively rapid motion of the excess proton on the molecular skeleton and/or preferential attachment to the ring carbon centers.

3.5. Methylation of thiophenol and thioanisole

Cooks and coworkers [16,17] proposed that alkylation of thiophenol and thioanisole occurs almost quantitatively on sulfur, not on the benzenic ring. We have then decided to use our two-step sequence of reactions to verify their findings.

In order to establish the methyl cation attachment site in thiophenol and thioanisole, we have first performed the CI of thioanisole using methyl iodide as the reagent gas. Under such conditions, the methylation of the neutral molecule is readily realized and the corresponding signal is observed at m/z 139. The low energy CA spectrum of these ions, using argon collision gas, features a loss of 15 Da as the major collision-induced dissociation. Use of perdeuterated methyl iodide could indicate the site of attachment of the methyl group on thioanisole. Indeed, in the case of a sulfur methylation, losses of CH_3^\bullet and CD_3^\bullet should be observed with identical efficiencies. The result of such an experiment is depicted in Fig. 7 and shown in Scheme 5. Clearly, the peaks associated with the losses of CH_3^\bullet (m/z 127) and CD_3^\bullet (m/z 124) are characterized by similar intensities in agreement with a sulfur methylation.

Chloromethane CI of 4-bromothiophenol leads to m/z 205 cations (^{81}Br -containing ions) corresponding to the methylated molecules. The low energy CA spectrum of these cations, performed in the quadrupole

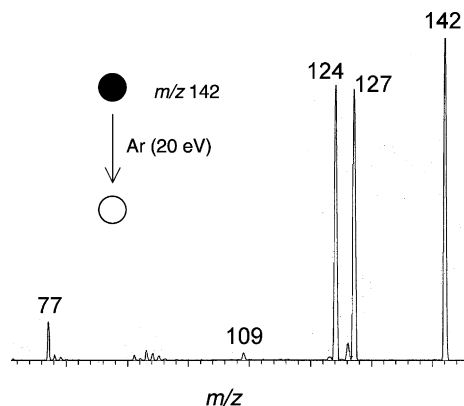
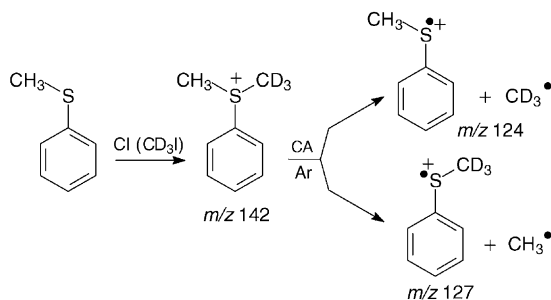


Fig. 7. CA spectrum (Ar, 20 eV) of thioanisole methylated by CD_3I in the CI source (m/z 142). The intensities of the signals corresponding to the collision-induced fragments are amplified by a factor 30.

cell with argon as the target, is shown in Fig. 8a. Debromination is by far the most intense reaction, and the MS/MS/MS spectrum, identical to the spectrum depicted in Fig. 5b, unambiguously indicates that thioanisole ions are produced in this experiment. As evidenced by Fig. 6, an hydrogen scrambling is likely to precede the fragmentation and, once the proton is introduced into the *ipso*-carbon position relative to the bromine, the debromination readily occurs (Scheme 6, Table 2).

Methylation of 4-bromothiophenol under methyl chloride CI conditions followed by low energy collisional activation of the methylated molecules (m/z 217) in the quadrupole collision cell gives rise to the CA spectrum shown in Fig. 8b. In contrast to the



Scheme 5.

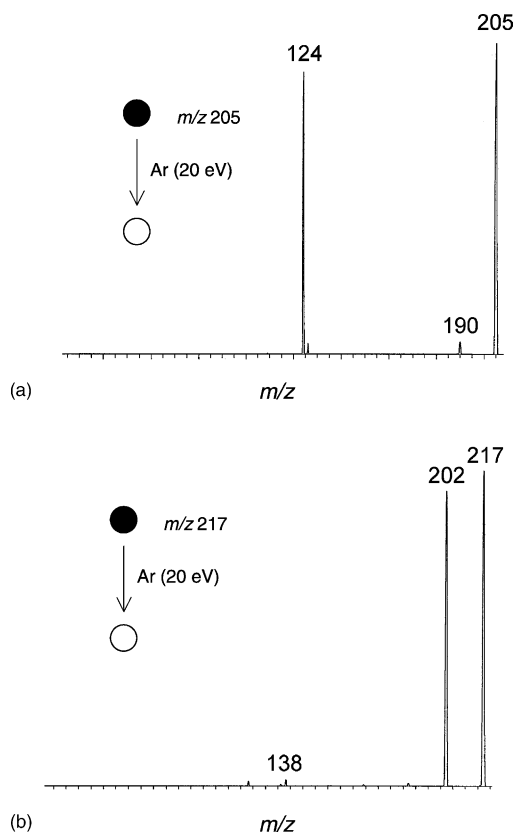
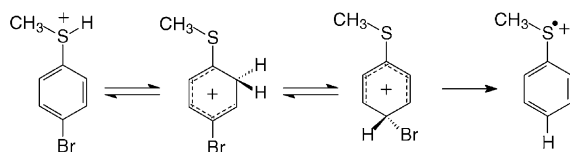


Fig. 8. CA spectra (Ar, 20 eV) (a) of methylated 4-bromothiophenol (m/z 205, ^{81}Br -containing ions to avoid interferences) (fragment ion peaks amplified by a factor 15) and (b) of methylated 4-bromothioanisole (m/z 217) (fragment ion peaks amplified by a factor 5).

thiophenol case, the loss of bromine is only marginally observed (about 1%) and is replaced by a prominent loss of a methyl group (m/z 202 cations). Although the loss of bromine was observed, the relative intensity of the corresponding signal precludes any further collision processes. The contrasting behavior upon



Scheme 6.

collisional activation of both methylated bromothiophenol and methylated bromothioanisole, respectively debromination viz. demethylation, is consistent with the calculated PES depicted in Fig. 6. Sulfonium ions bearing a hydrogen atom on sulfur are prone to isomerize into a ring protonated species. As a consequence, the production of conventional ions does not necessarily imply a regiospecific ring protonation.

Calculated results given in Tables 1 and 3 quantitatively support this proposal. In thiophenol, a more favored methylation at sulfur is already noticed, namely by 9 kJ mol^{-1} with respect to a C_4 -methylation. The S-methylation preference is further enhanced in thioanisole where the energy gap is enlarged up to 31 kJ mol^{-1} . In going from thiophenol to thioanisole, the methyl effect results in an increase of 57 kJ mol^{-1} of the methyl cation affinity (MCA) at sulfur. For the latter quantity, we would suggest the following values: MCA (thiophenol) = $397 \pm 12 \text{ kJ mol}^{-1}$ and MCA (thioanisole) = $454 \pm 12 \text{ kJ mol}^{-1}$.

4. Concluding remarks

In the present combined mass spectrometric and quantum chemical study, we have endeavored to determine the preferential site of protonation and methylation in thiophenol, thioanisole and their halogenated derivatives in the gas phase. The ring carbon atom in the *para* position with respect to the thiohydroxy group, C_4 , is found to be the most favored protonation site in the parent thiophenol, thioanisole, and in their *ortho*- and *meta*-monohalogenated derivatives. In the *para*-halogeno compounds, while fluorine and chlorine modify the pattern giving a preferential C_2 -protonation, bromine upholds a C_4 protonation. Nevertheless, experimentally speaking, it was not possible to unambiguously confirm the protonation site due to the (i) too weak difference between sulfur and ring proton affinities, especially in the case of thioanisole, and (ii) easy isomerization by proton motion of the different protonated molecules.

However, regarding methylation process, it is confirmed that in all cases methyl cation consistently

prefers to be bound to the sulfur atom rather than to the phenyl ring. Due to the ease with which the excess proton circulates around the heavy atom skeleton, fragmentation of the protonated halogeno species, by either demethylation or debromination, invariably yields the more stable classical thiophenol or thioanisole radical cations. Non-conventional or distonic ion isomers have not been detected in the various MS/MS/MS experiments.

A few useful thermochemical parameters have also been evaluated as follows: PA (thiophenol) = $812 \pm 10 \text{ kJ mol}^{-1}$, PA (thioanisole) = $839 \pm 10 \text{ kJ mol}^{-1}$, MCA (thiophenol) = $397 \pm 12 \text{ kJ mol}^{-1}$ and MCA (thioanisole) = $454 \pm 12 \text{ kJ mol}^{-1}$. Numerous results showed that the deviations of proton affinities computed at the B3LYP/6-311++G(d,p) level, with respect to well-established experimental values, amount to at most $\pm 10 \text{ kJ mol}^{-1}$. Regarding the methyl cations affinities, much less experimental values are actually available for comparison, therefore, we adopt a more conservative error bars of $\pm 12 \text{ kJ mol}^{-1}$. The available experimental value of 873 kJ mol^{-1} for the PA of thioanisole is apparently overestimated.

Acknowledgements

The Leuven group is indebted to the KU-Leuven Research Council (GOA-program) for financial support. The Mons laboratory thanks the "Fonds National de la Recherche Scientifique" for its contribution to the acquisition of a large scale tandem mass spectrometer, Micromass AutoSpec 6F. P.G. also thanks the FNRS for a post-doctoral fellowship.

References

- [1] Z.B. Alfassi, S-Centered Radicals, Chichester, UK (1999).
- [2] G. Scott, Atmospheric Oxidation and Antioxidants, vols. I and II, Elsevier, Amsterdam, The Netherlands, 1993.
- [3] T.V. DeCollo, W.J. Lees, *J. Org. Chem.* 66 (2001) 4244.
- [4] R. Hermann, G. Dey, S. Naumov, O. Brede, *Phys. Chem. Chem. Phys.* 2 (2000) 1213.
- [5] R. Hermann, S. Naumov, G.R. Mahalaxmi, O. Brede, *Chem. Phys. Lett.* 324 (2000) 265.
- [6] O. Brede, G.R. Mahalaxmi, S. Naumov, W. Naumann, R. Hermann, *J. Phys. Chem. A* 105 (2001) 3757.
- [7] S. Kimura, E. Bill, E. Bothe, T. Weyhermuller, K. Wieghardt, *J. Am. Chem. Soc.* 123 (2001) 6025.
- [8] A.G. Larsen, A.H. Holm, M. Roberson, K. Daasbjerg, *J. Am. Chem. Soc.* 123 (2001) 1723.
- [9] A. Rauk, D. Yu, D.A. Armstrong, *J. Am. Chem. Soc.* 120 (1998) 8848.
- [10] F.G. Bordwell, Z.M. Zhang, A.V. Satish, J.P. Cheng, *J. Am. Chem. Soc.* 116 (1994) 6605.
- [11] C. Walford, R.F.W. Jackson, N.H. Rees, W. Clegg, S.L. Heath, *J. Chem. Soc. Chem. Commun.* (1997) 1855.
- [12] S.S. Kim, A. Tuchkin, C.S. Kim, *J. Org. Chem.* 66 (2001) 7738.
- [13] C.A. Bunton, N.D. Gillitt, *J. Phys. Org. Chem.* 15 (2002) 29.
- [14] S. Ozaki, S. Watanabe, S. Hayasaka, M. Konuma, *Chem. Commun.* (2001) 1654.
- [15] K. Nishimura, M. Ono, Y. Nagaoka, K. Tomioka, *J. Am. Chem. Soc.* 119 (1997) 12974.
- [16] K.V. Woods, D.J. Burinsky, D. Cameron, R.G. Cooks, *J. Org. Chem.* 48 (1983) 5236.
- [17] S.J. Pachuta, I. Isem-Flecha, R.G. Cooks, *Org. Mass Spectrom.* 21 (1986) 1.
- [18] N. Solca, O. Dopfer, *Chem. Phys. Lett.* 342 (2001) 191.
- [19] O. Tischenko, N.N. Pham-Tran, E.S. Kryachko, M.T. Nguyen, *J. Phys. Chem. A* 105 (2001) 8709.
- [20] H.T. Le, R. Flammang, P. Gerbaux, G. Bouchoux, M.T. Nguyen, *J. Phys. Chem. A* 105 (2001) 11582.
- [21] R. Flammang, M. Barbieux-Flammang, E. Gualano, P. Gerbaux, H.T. Le, M.T. Nguyen, F. Turecek, S. Vivekananda, *J. Chem. Phys. A* 105 (2001) 8579.
- [22] H.T. Le, R. Flammang, M. Barbieux-Flammang, P. Gerbaux, M.T. Nguyen, *Int. J. Mass Spectrom.* 217 (2002) 45.
- [23] R. Flammang, M. Barbieux-Flammang, E. Gualano, P. Gerbaux, H.T. Le, F. Turecek, M.T. Nguyen, *Int. J. Mass Spectrom.* 217 (2002) 65.
- [24] H.T. Le, P. Gerbaux, R. Flammang, M.T. Nguyen, *Chem. Phys. Lett.* 323 (2000) 71.
- [25] R.H. Bateman, J. Brown, M. Lefevre, R. Flammang, Y. Van Haverbeke, *Int. J. Mass Spectrom. Ion Processes* 115 (1992) 205.
- [26] R. Flammang, Y. Van Haverbeke, C. Braybrook, J. Brown, *Rapid Commun. Mass Spectrom.* 9 (1995) 795.
- [27] M.J. Frisch, G.W. Trucks, H.B. Schlegel, P.M.W. Gill, B.G. Johnson, M.A. Robb, J.R. Cheeseman, T.A. Keith, G.A. Petersson, J.A. Montgomery, K. Raghavachari, M.A. Al-Laham, V.G. Zakrzewski, J.V. Ortiz, J.B. Foresman, C.Y. Peng, P.Y. Ayala, M.W. Wong, J.L. Andres, E.S. Replogle, R. Gomperts, R.L. Martin, D.J. Fox, J.S. Binkley, D.S. DeFrees, J. Baker, J.P. Stewart, M. Head-Gordon, C. Gonzalez, J.A. Pople, *Gaussian 94*, Rev. C3, Gaussian Inc., Pittsburgh, PA, 1995.
- [28] (a) A.D. Becke, *J. Chem. Phys.* 98 (1993) 1372;
(b) C. Lee, W. Yang, R.G. Parr, *Phys. Rev. B* 37 (1988) 785.
- [29] R. Flammang, A. Maquestiau, *Chim. Nouv.* 5 (1987) 516.

- [30] D.J. Lavorato, J.K. Terlouw, G.A. McGibbon, T.K. Dargel, W. Koch, H. Schwarz, *Int. J. Mass Spectrom.* 179 (1998) 7.
- [31] M.T. Nguyen, T.L. Nguyen, H.T. Le, *J. Phys. Chem. A* 103 (1999) 5758.
- [32] H.T. Le, T.L. Nguyen, D. Lahem, R. Flammang, M.T. Nguyen, *Phys. Chem. Chem. Phys.* 1 (1999) 755.
- [33] E.P. Hunter, S.G. Lias, *J. Phys. Chem. Ref. Data* 27 (1998) 413.
- [34] NIST Webbook, <http://webbook.nist.gov/chemistry>.
- [35] J.C. Schwartz, A.P. Wade, C.G. Enke, R.G. Cooks, *Anal. Chem.* 62 (1990) 1809.